Marine snow latitudinal distribution in the equatorial Pacific along 180 degrees

G Gorsky, R Le Borgne, M Picheral, L Stemmann

Marine snow latitudinal distribution in the equatorial Pacific along 180°

Gabriel Gorsky

Observatoire Océanologique, Laboratoire d'Océanographie de Villefranche-sur-Mer, CNRS/UPMC, Villefranche sur mer, France

Robert Le Borgne

Centre Institut de Recherche pour le Développement, Nouméa, New Caledonia

Marc Picheral and Lars Stemmann

Observatoire Océanologique, Laboratoire d'Océanographie de Villefranche-sur-Mer, CNRS/UPMC, Villefranche sur mer, France

Received 23 July 2001; revised 11 February 2003; accepted 7 March 2003; published 26 November 2003.

[1] Marine snow (MS) distribution from the surface to 1000 m depth was determined in the equatorial Pacific using the underwater video profiler during the Etude du Broutage en Zone Equatoriale cruise in fall 1996. The latitudinal transect was carried out at 17 stations along the 180° meridian from 8°S to 8°N during a cold phase of El Niño-Southern Oscillation. Higher MS concentrations were found below the equatorial zone than poleward. At the equator the estimated integrated MS carbon m^{-2} in the upper kilometer was 5.7 g m^{-2}, while both southward and northward (between 1° and 8°) the mean integrated MS carbon was about 2.7 g. m^{-2}. In the upper 50 m the MS carbon was twofold lower than the combined carbon of autotrophic and heterotrophic protists and four times lower than the mesozooplankton carbon biomass, both measured concurrently during the cruise. Different water bodies had different MS content. The highest concentrations were found in the South Equatorial Current, the South Equatorial Counter Current, and the North Equatorial Countercurrent. Tropical waters at the south in the South Subsurface Countercurrents and the warm northern superficial waters had the lowest MS biomass. Mechanistically, a latitudinal "conveyor belt", a poleward divergence of upwelled waters that return to the equator after being downwelled at north and south convergent zones, may partially explain the vertical distribution of particulate matter observed during the studied period. *INDEX TERMS:* 4805 Oceanography: Biological and Chemical: Biogeochemical cycles (1615); 4806 Oceanography: Biological and Chemical: Carbon cycling; 4283 Oceanography: General: Water masses; 4294 Oceanography: General: Instruments and techniques; 4863 Oceanography: Biological and Chemical: Sedimentation; *KEYWORDS:* equatorial Pacific, carbon cycling, particulate organic matter, marine snow, latitudinal advection, Underwater Video Profiler

Citation: Gorsky, G., R. Le Borgne, M. Picheral, and L. Stemmann, Marine snow latitudinal distribution in the equatorial Pacific along 180°, *J. Geophys. Res.*, *108*(C12), 8146, doi:10.1029/2001JC001064, 2003.

1. Introduction

[2] The equatorial Pacific is the main natural source of atmospheric CO_2 in the oceans [*Tans et al.*, 1990] but at the same time, it also acts as an important CO_2 sink because of its major contribution to global new production [*Chavez and Barber*, 1987; *Chavez and Toggweiler*, 1995]. Both new production and CO_2 evolution mechanisms are closely linked to equatorial upwelling, which varies temporally and spatially. To the west is the warm pool region, characterized by an oligotrophic stratified structure. The zonal boundary between oligotrophic and upwelling regions is influenced by interannual variations associated with the El Niño-Southern Oscillation (ENSO) cycle [*Picaut et al.*, 1996; *Le Borgne et al.*, 2003]. On shorter timescales, community structure, functioning of the upwelling ecosystem and thus the downward export of the upper layer primary productivity respond to seasonal cycles, equatorial Kelvin waves and tropical instability waves [*Dunne et al.*, 2000; *Eldin and Rodier*, 2003; *Le Borgne et al.*, 2003].

[3] Particles are responsible for the vertical transport of material in the ocean. Marine snow particles (i.e., macroscopic marine aggregates >500 μm) are ubiquitous and may dominate the total mass sinking flux because of their abundance and rapid settling rates [*Asper*, 1987]. Ranging from pure phytoplankton flocks to amorphous detritus and zooplankton remains [*Alldredge and Silver*, 1988], particles are of different sizes and origins and subjected to different kinds and degrees of water column processing. Their sinking trajectories and dissolution/aggregation processes are there-

0148-0227/03/2001JC001064

fore difficult to interpret. Nonetheless, *Walsh and Gardner* [1992] demonstrated that sediment trap estimates of carbon fluxes in the equatorial Pacific were proportional to the concentration and size distribution of large aggregates.

[4] Phytoplankton biomass in the equatorial Pacific upwelling zone is characterized by latitudinal gradients with the highest values being generally observed at or near the equator [*Chavez*, 1989; *Brown et al.*, 2003; *Le Bouteiller et al.*, 2003]. The fate of the phytoplankton in this region is an important issue with respect to the importance of the biological pump. According to *Dam et al.* [1995] and *Gaudy et al.* [2003], a large proportion of the carbon ingested by mesozooplankton is not phytoplankton. Most of the direct grazing of primary producers is done by microzooplankton [*Landry et al.*, 1995; *Le Borgne and Landry*, 2003]. Organic aggregates form as the result of grazing and detrital processes acting on the phytoplankton. While rapidly sinking dense fecal pellets can be quantified from sediment traps [*Fowler and Knauer*, 1986], this is not the case for the porous, marine snow like particles (MS). Direct in situ measurements of the standing stocks of MS particles are difficult because of their fragile nature, but *Alldredge* [1998] has shown that particle mass is a function of size and that elemental compositions are similar regardless of origin, composition or season of collection. Imaging methods therefore provide an alternative in situ approach to quantifying the abundances and distribution patterns of undisturbed large particles. Although several still and video camera systems have been developed for this purpose [*Honjo et al.*, 1984; *Asper*, 1987; *Gardner and Walsh*, 1990; *MacIntyre et al.*, 1995; *Walsh et al.*, 1997; *Gorsky et al.*, 1992, 2000], studies applying these imaging approaches across system gradients in the oceans are still relatively few.

[5] The French Etude du Broutage en Zone Equatoriale (EBENE) cruise, conducted during a cold ENSO period in 1996 in the framework of the international JGOFS program, provided an opportunity to study large particulate matter as part of a broad investigation of food web interactions in the equatorial Pacific upwelling region. In this paper, we report on the latitudinal distribution of MS in the first kilometer of the equatorial Pacific along the 180° meridian from 8°S to 8°N.

2. Materials and Methods

[6] Data on the vertical distribution of particulate matter (>460 μm) were collected with the Underwater Video Profiler (UVP) [*Gorsky et al.*, 1992, 2000, 2002] during the French EBENE cruise (23 October to 12 November 1996) onboard R/V *L'Atalante*. The cruise consisted of a sampling transect along the 180° dateline, with stations being made at every degree of latitude between 8°N and 8°S.

2.1. Underwater Video Profiler

[7] The UVP (model #3), developed at the Observatoire Oceanographique de Villefranche sur mer, France is a multi-array instrument composed of the following sensors: Exavision XC 644 black and white video camera equipped with a 12 mm focal distance lens, a Sony video recorder, a fluorometer and a nephelometer (both Chelsea Instruments Ltd.) coupled to a Seabird 19 CTD probe. Particles contained in a known volume of water (1.3 l), are illuminated by two 54 W Chatwick Helmut stroboscopes delivering a collimated light beam. Environmental data gathered by the other sensors is recorded simultaneously. The system is independently powered by 24V batteries and is controlled by a Texas 370 microprocessor. A complete 0–1000 m vertical profile with the UVP system consists of approximately 25,000 images, taken at a 1m s^{-1} lowering speed and an acquisition rate of 25 images s^{-1} (http://www.metal-process.com).

2.2. Data Analysis

[8] Data are processed by two custom-built programs. The first one, written in Visual C++ (Microsoft), digitizes the images without compression and performs the image analysis, saving the number of particles per image and their attributes to an ASCII file. The second program (MATLAB, Scientific Software) is used for data processing and editing. Particles are enumerated and their individual cross-sectional areas, lengths and Equivalent Spherical Diameters (ESD) determined. Particle volumes are obtained from ESDs, and the individual aggregate volumes are converted into carbon biomass estimates using the dry weight (DW) to aggregate size relationship of *Alldredge and Gotchalk* [1989] and the C:DW ratio of 0.2 found for large refractory aggregates [*Alldredge*, 1998].

[9] Particle abundances and size spectra are averaged, respectively, for 5 and 20-m thick layers. The metric surface (Y) as a function of the pixel surface (X) can be expressed by the following equations obtained from laboratory calibrations [see *Gorsky et al.*, 2000]:

$$12\text{ mm}: Y = 0.02\,X^{1.137}, \qquad R^2 = 0.873$$

[10] Data processing only applies to the portion of the vertical profile where images display a constant dark background since sunlight interferes with the collimated light beam. Therefore the analysis starts at depth where such interference becomes negligible. This was not a problem for most of the station profiles, which were sampled at night. However, sunlight effects limited the analyses to depths below 90 m at 4°S and 5°N, below 25 m at 2°S, and below 110 m at 7°S and 2°N. Because of a power failure, data at 8°S were acquired only from the surface to 160 m.

[11] With the exception of the missing depth ranges given above, MS size distributions were averaged for 6 depth strata (0–50, 50–125, 125–250, 250–500, 500–750, and 750–1000 m) at each of the 17 transect stations. The hierarchical flexible clustering was performed on a matrix of Kolmogorov distances among these size distributions [*Legendre and Legendre*, 1984]. At a distance of 45, three types of size distributions could be discriminated. This distance can be used for the detection of variation between distributions. Thus the distributions of the "large particles" group is characterized by higher frequency of particles >0.5 mm, compared to the other two distributions. Particles <0.5 mm dominate the group of "small particles" [see *Stemmann et al.*, 2000].

3. Results

3.1. Water Circulation and Marine Snow Distributions

[12] As described by *Eldin and Rodier* [2003], the South Equatorial Current (SEC) was flowing westward at 180°, between 5°S and 4°N, during the EBENE cruise, and the

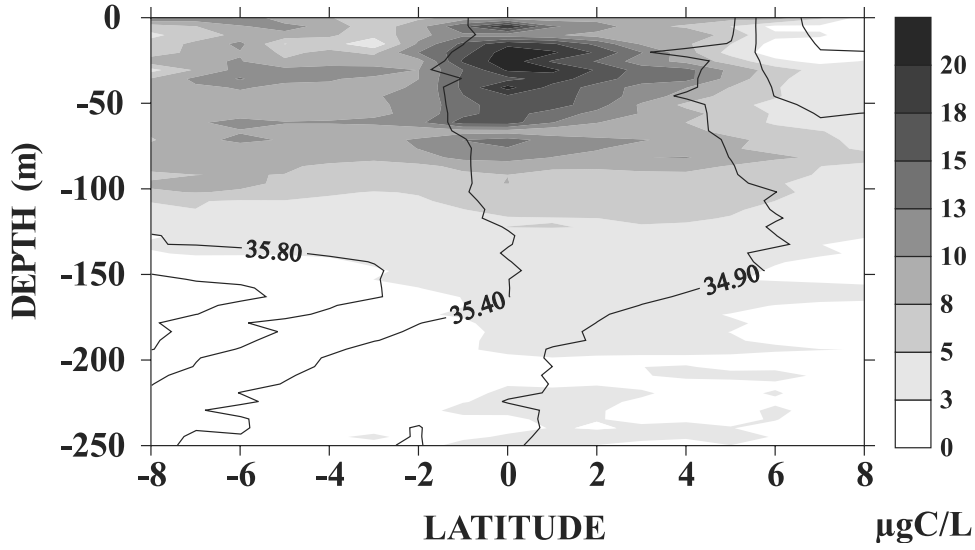

Figure 1. Latitudinal distributions of marine snow carbon mass (gray scale) and the salinity field (psu) in the upper 250 m of the EBENE equatorial transect.

North Equatorial Countercurrent (NECC) flowed eastward, north of 4°N. Subsurface flow consisted of the eastward flowing Equatorial Under-Current (EUC), centered at the equator below 100 m. The South and North Subsurface Countercurrents (SSCC, NSCC) also flowed eastward below 200 m south of 6°S and north of 2°N, respectively. The maximum velocity of the SEC was 90 cm/s (north of the equator), while the highest velocity of the EUC was 60 cm/*s*. The Equatorial Intermediate Current (EIC) flowed westward below the EUC between 0° and 2°N. The South Equatorial Counter Current (SECC) was observed south of 5°S and was associated with the deepening of the warm surface waters [*Eldin and Rodier*, 2003]. A tongue of high-salinity and particle-depleted tropical water (TW) was present in the thermocline, south of 1°S (Figure 1).

[13] Isotherm gradients were influenced by the geostrophic zonal circulation. Near the surface, temperature values were lowest at the equator and highest on both ends of the latitudinal transect. At the equator, the 28°C isotherm that defines the top of the upper thermocline extended almost to the surface because of upwelling. Both turbidity and fluorescence values were highest in the equatorial zone. Fluorescence maxima deepened poleward, from 50 m at the equator to about 80 m at 8°S and below 100 m at 8°N (data not shown). MS concentrations peaked near the equator at the surface and also in the underlying deep layers (Figure 2).

[14] MS concentrations are compared in Table 1 for the different water types, selected according to the flow fields described by *Eldin and Rodier* [2003]. MS concentrations were high in the lower part of the SECC, above the TW. Particulate densities were very low in the saline TW, and remained so in the SSCC. Subsurface minimum concentrations of MS were observed in the EUC, whereas the highest midwater values, exceeding one third of surface

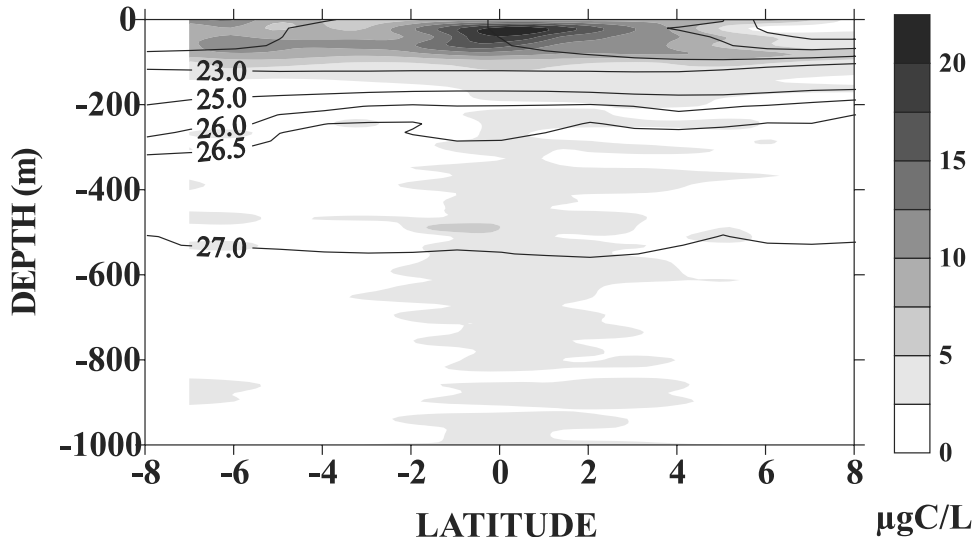

Figure 2. Vertical distributions of >460-µm marine snow particles (µg C L^{-1}) in relation to the 0–100 m density field (sigma-θ) along the EBENE equatorial transect. Data below 160 m are missing at 8°S.

Table 1. Mean Concentrations, Volumes (ppm), and Carbon Weights ($\mu g\ L^{-1}$) of Marine Snow (MS) Particles in Different Water[a]

	7°S, SECC	S.D.	6°S, TW	S.D.	3°S, SSCC	S.D.	0° EUC	S.D.	1°N, Upper SEC	S.D.	1°N, Lower SEC	S.D.	3°N, NSCC	S.D.	6°N, NECC	S.D.	8°N, Oligo	S.D.
Depth, m	110–150		160–200		250–300		150–200		0–100		250–300		200–300		50–150		0–50	
Mean Number, L^{-1}	4.11	1.65	0.62	0.33	1.24	0.51	3.10	0.93	9.95	5.77	3.25	1.07	2.74	0.94	3.28	1.84	1.68	0.99
Mean Volume, ppm	0.91	0.22	0.11	0.10	0.16	0.11	1.15	1.48	2.35	2.42	0.62	0.27	0.58	0.38	0.53	0.34	0.44	0.36
Mean Carbon Weights, $\mu g\ L^{-1}$	4.72	1.64	0.68	0.39	1.20	0.58	3.71	1.50	11.32	6.98	3.65	1.29	3.07	1.07	3.47	1.98	2.05	1.27

[a]SECC, South Equatorial Counter Current (data above 110 m were not available); TW, Tropical Waters; SSCC, South Subsurface Counter Current; EUC, Equatorial Undercurrent; EIC, Equatorial Intermediate Current; SEC, South Equatorial Current; NSCC, North Subsurface Counter Current; ECC, North Equatorial Counter Current; Oligo, warm northern surface waters (stations 6°N, 7°N and 8°N); and S.D., standard deviation. For detailed descriptions of the hydrological conditions, see *Eldin and Rodier* [2003].

values, were measured in the EIC around 300 m. MS concentrations were similar in the NSCC and the EUC. Warm surface waters north of 6°N displayed lower concentrations of particles than deeper in the NECC. Overall, equatorial stations had higher concentrations of large particles (size distributions were determined using the hierarchical flexible clustering method [see *Stemmann et al.*, 2000]). Large aggregates were observed at the station 6°S and in the superficial oligotrophic waters of the stations 7°N and 8°N, but in low numbers (1–2 aggregates l–1). Elsewhere, the smaller MS size classes prevailed. In subsurface layers, MS concentrations were high in the equatorial zone and in the SECC and NECC.

[15] Comparison of MS concentrations in different layers against the mean value calculated for the whole transect shows that only the equatorial MS values were consistently higher in concentrations and volume than the latitudinal mean. All values obtained at stations 5°S and 7°N were lower than the latitudinal mean. At 6°S, the concentration and volume were higher than the mean in the upper 150 m, but not in below. Globally, the stations south of the equator (5°–2°S) displayed a deficit when compared to the MS latitudinal mean. Northern stations (1°–3°N) had MS concentrations higher than the mean (Figure 3). Station 4°N separated the near equatorial stations with higher MS concentration from peripheral stations with low superficial concentration. The convergence zone between 4 and 5°N was also the site of accumulation and downward export of the autotrophic and heterotrophic microbial biomass [*Brown et al.*, 2003].

[16] Four main hydrographic patterns can be discerned when T/S profiles of the sampled stations are compared (not shown here) [*Eldin and Rodier*, 2003]. One characterizes stations south of the equator, the second is the equatorial station, the third includes northern stations near the equator, and the three extreme northern stations comprise the fourth. Examining the distributions of particulate carbon from the surface to 1000 m along the cross-equatorial transect, it appears that the relatively high values are grouped in a narrow temperature and salinity range. Concentrations exceeding 15 $\mu g\ C\ L^{-1}$ were found in the surface layer at only three stations (1°S, 0° and 1°N), and the highest MS concentrations were distributed along a salinity gradient extending from 35 to 35.5 (Figure 4). Station 6°S showed high MS concentrations only in the upper 150 m. Beneath this depth, in the high-salinity tropical water (TW), the particle load was much lower, and the resulting integrated MS carbon was equivalent to the corresponding northern stations.

3.2. Latitudinal Size Distribution

[17] Generally, decreases in MS particle abundances are coupled with the increasing individual particle size [*Stemmann et al.*, 2000]. In the present study, large particles were found in the upper 250 m, mostly between 2°S and 4°N (Figure 5). Abundance distributions were often negatively correlated with the size at individual stations (c.f. stations 7° and 8°N). However, around the equator (from 1°S to 1°N), the abundance of large particles was high in the superficial layers.

4. Discussion

4.1. MS Depth Distributions

[18] Interactions between the different water masses may influence the fate of surface produced biogenic matter. Diatoms, for instance, have the potential to form flocs that sink eventually to deeper layers [*Alldredge and Gotschalk*, 1989; *Kiorboe et al.*, 1998]. During the EBENE cruise, *Brown et al.* [2003] observed the highest accumulation of large diatoms in surface waters near the equator. The abundance of large particles measured by the UVP was also highest in the equatorial surface layer (Figure 5). Our results show, however, that the MS concentration decreased in the EUC, forming a discontinuity between the near-surface and deep layers. Such a discontinuity and the low zooplankton biomass below 100 m [*Le Borgne et al.*, 2003], raise the following question: what processes influence the vertical distribution of marine snow?

[19] *Walsh et al.* [1997] proposed a conceptual model in which the equatorial upwelling results in a poleward divergent flow of near-surface waters. Following a circular pattern, surface flow reaches northern and southern convergence zones and returns to the equator in the deeper layers. The effects of frontal subduction are difficult to measure directly but may be suggested by the spatial distribution of chlorophyll pigments [*Kadko et al.*, 1991; *Send et al.*, 1999; *Videau et al.*, 1994] or by the vertical distribution of large particulates. For instance, *Gorsky et al.* [2002] found that fast sinking particles, such as large aggregates, sediment near the site of their production, while small and porous aggregates can be advected substantial distances before they sink.

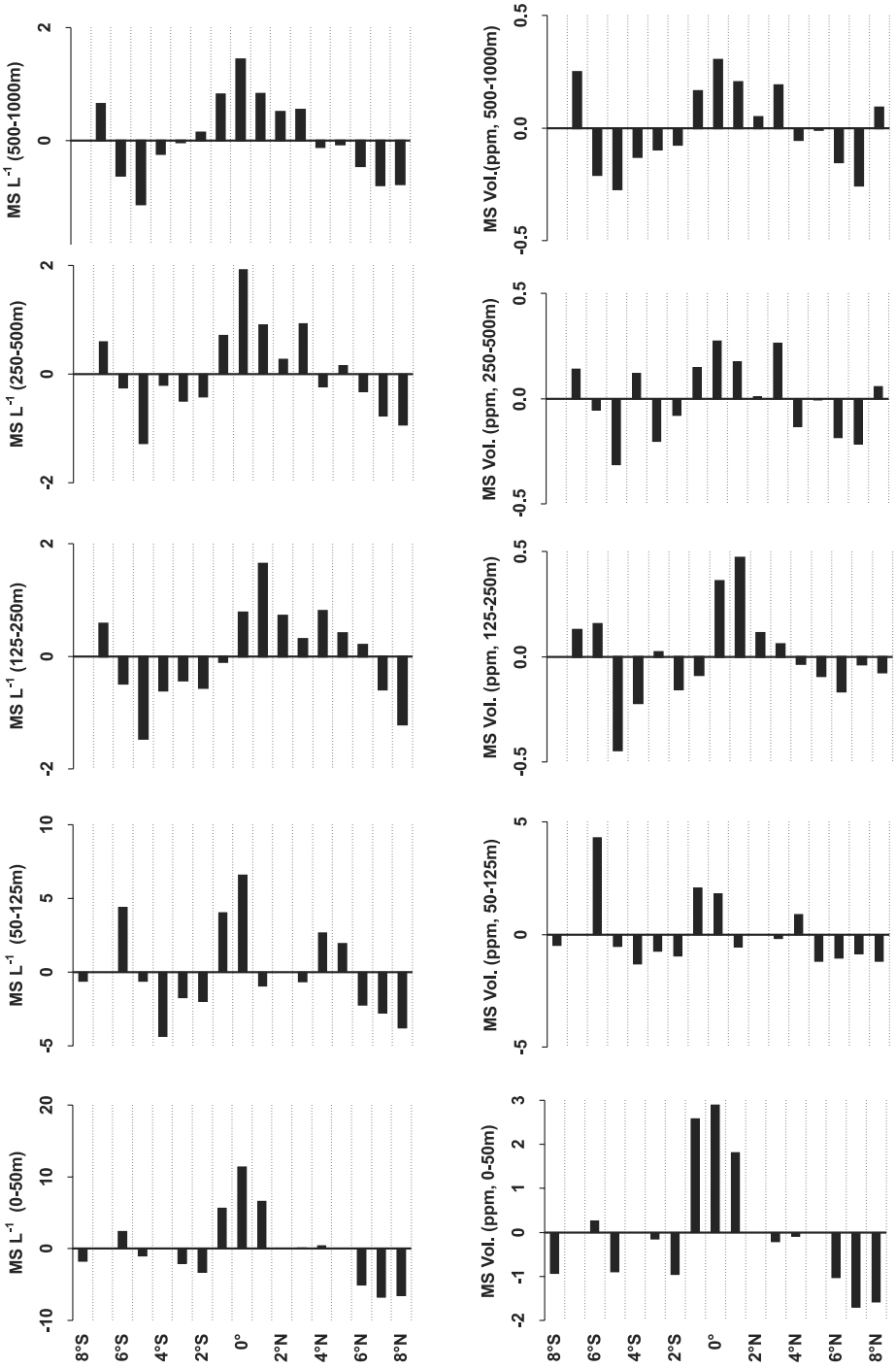

Figure 3. Variability of marine snow (MS) concentrations in different depth strata around the latitudinal mean (=0) for EBENE equatorial transect.

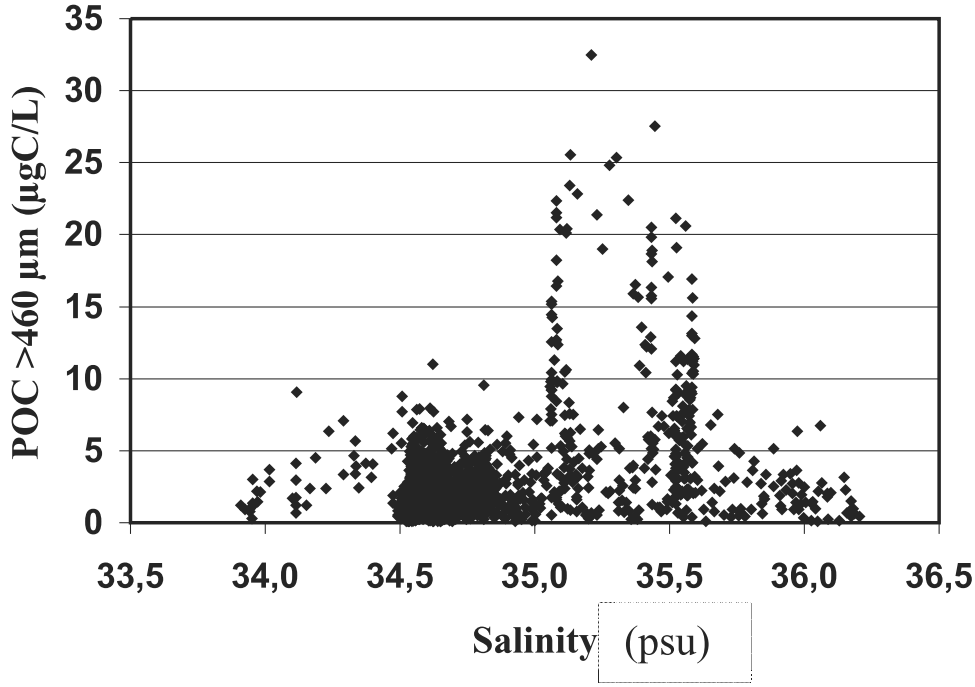

Figure 4. Carbon biomass of marine snow (MS) particles, as estimated by the Underwater Video Profiler, as a function of salinity along the EBENE latitudinal section.

[20] Two convergence zones are evident in the current profiles of the EBENE equatorial cross section provided by *Eldin and Rodier* [2003]. One is in the vicinity of 4°N, where *Eldin and Rodier* [2003] found an anomalous deepening of the surface layer corresponding to a horizontal convergence between a strong NECC north of 4°–5°N and the SEC (westward flow between 5°S and 4°N). A second convergence appears at 5°S between the SEC and the SECC. The two convergences, marked by a deepening of the thermocline at 4°N and 5°S, may induce an advective transport of organic matter. The meridional surface flows are the results of upwelling and poleward divergence occurring between the EUC and SEC [*Walsh et al.*, 1997]. This surface flow is mixed and downwelled at convergence zones and returns as a subsurface return flow to the equator. Mechanistically, this subsurface return flow could act as a latitudinal conveyor belt, transporting part of the advected surface biological production back to deeper equatorial layers.

[21] According to *MacIntyre et al.* [1995], turbulence may contribute to the accumulation of small particles. In fall 1996, biological production peaked at the equator. *Brown et al.* [2003] studied the abundance and composition of the microbial community on the EBENE equatorial cross section. The accumulation of photosynthetic and heterotrophic biomass observed by the latter authors between 4° and 5°N could fuel the particle aggregation processes during the downwelling of water masses at the convergent fronts. Large aggregates could then be produced continuously during the advective transport back to the equatorial zone. Such a mechanism may explain the observed discontinuity in MS concentrations between the superficial and deeper equatorial layers (Figure 2) and the observed change in MS

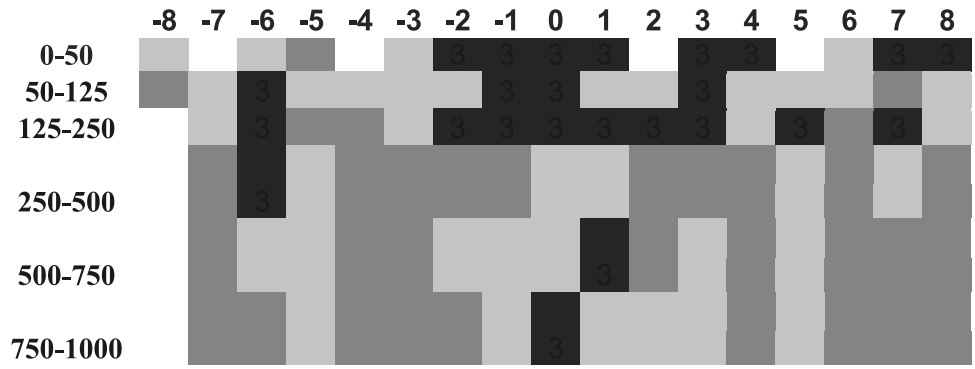

Figure 5. Latitudinal section of the relative proportions of large, medium, and small marine snow particles in different depth strata along the EBENE transect. Black rectangles, large particles; dark gray rectangles, medium-sized particles; light gray rectangles, the smallest size class particles; and white rectangles, missing data.

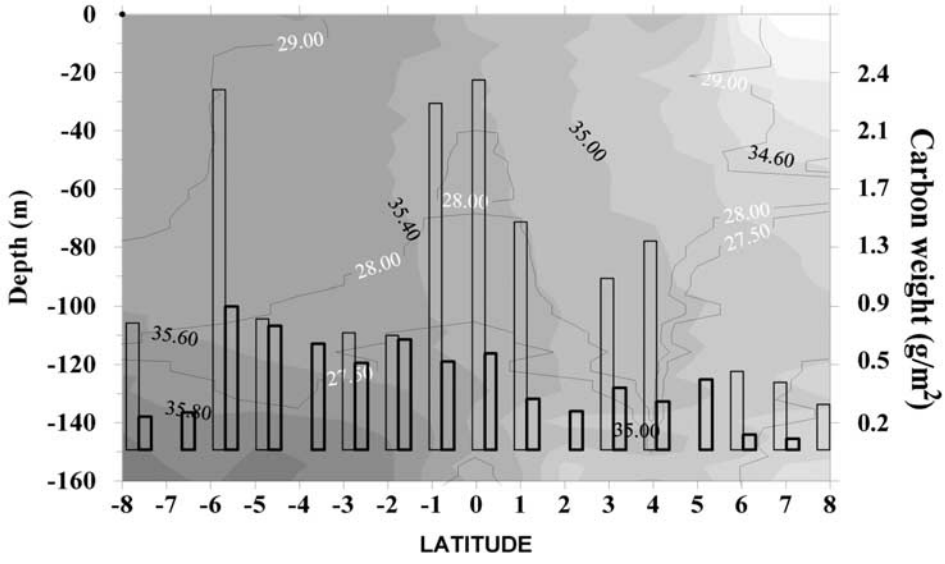

Figure 6. Depth-integrated (0–150 m) carbon estimates of marine snow particles (thin histograms) and mesozooplankton (thick histograms) relative to surface temperature (isolines with white labels) and salinity (contour plot, dark labels) fields along the EBENE transect.

vertical distribution at 4°N (Figure 3). On the other hand, the high concentration of MS in the upper 150 m at 6°S could be associated both with the frontal feature between the SEC and the SECC (Figure 6) and with the horizontal intrusion of the TW below 150 m limiting the vertical dilution of particles. Although weaker during the EBENE cruise, the southern convergence has been previously described as an active feature [*Radenac and Rodier*, 1996].

4.2. MS as a Carbon Reservoir

[22] MS carbon content was calculated for each individual particle detected optically using the relationships of *Alldredge and Gotschalk* [1988] and *Alldredge* [1998]. Results obtained by different imaging systems under similar conditions are comparable [*MacIntyre et al.*, 1995; *Jackson et al.*, 1997]. Our results show that MS standing stock averaged 2.7 gC m^{-2} in the upper kilometer of the water column in the southern part of the transect, 5.6 gC m^{-2} at the equator and 2.7 gC m^{-2} at the northern stations (Table 2). MS concentrations peaked in surface waters near the equator and also in the underlying deep layers (Figure 2). In the upper 50 m, the combined average autotrophic and heterotrophic carbon biomass associated with <200-μm protists was about twofold higher than the MS carbon mass and about four times higher than mesozooplankton carbon [*Brown et al.*, 2003; *Le Borgne et al.*, 2003].

[23] Diel vertical migration of mesozooplankton (200–2000 μm) was investigated during the two long-term stations, the equator and 3°S, during the EBENE cruise [*Le Borgne et al.*, 2003]. Over the 0–400 m depth range, day/night differences in mesozooplankton biomass were not significant. In the equatorial HNLC zone, mesozooplankton were concentrated in the superficial 100 m layer and consisted mainly of surface living, nonmigratory species [*Le Borgne et al.*, 2003]. Although the carbon content of the heterotrophic microbial community below 100 m was not measured, the decrease of the autotrophic particles and zooplankton carbon mass with depth emphasizes the importance of the MS as particulate carbon pool in the ocean's interior (Table 2).

[24] As a consequence of the surface distribution and reduced diel migrations of mesozooplankton in the HNLC water column, the "active" export of carbon from the euphotic zone is relatively low. Therefore the latitudinal "conveyor belt" as proposed by *Walsh et al.* [1997] may play a nonnegligible role in the vertical flux of organic matter to deeper equatorial layers. Because of the complex climatic forcing and zonal water circulation more data are necessary to support the proposed circulation mechanism for MS particles.

5. Conclusions

[25] As for most biological parameters, the equatorial upwelling zone is marked by a near-surface biomass maximum in marine snow particles. However, because of the strong shear between the SEC and the EUC and to the upwelling divergence, there is a discontinuity between MS

Table 2. Mean Integrated Carbon Weight (in mg C m^{-2}) of Marine Snow (MS) Particles in the Southern, Equatorial, and Northern Stations of the Latitudinal Transect for Each Depth Layer[a]

Depth, m	South	S.D.	0°	North	S.D.
50–0	595	482	1157	431	319
100–50	443	242	875	298	158
150–100	167	74	288	178	98
200–150	68	23	192	139	65
400–200	317	107	700	428	149
1000–400	1117	840	2464	1244	913
Total 0–1000	2707		5676	2718	

[a]S.D. is standard deviation. MS carbon values (in mg C m^{-2}) are calculated from equivalent spherical diameters following *Alldredge and Gotschalk* [1989] and *Alldredge* [1998].

concentrations in the surface and deep waters. Our hypothesis for such a discontinuity is that part of the equatorial surface MS, as well as other biogenic matter that ultimately aggregates into large particulates, is transported poleward to the southern and northern convergence zones, where it sinks and is transported back to the equator by deep currents. If this mechanism is correct, it provides another example of the importance of latitudinal effects on production processes in the equatorial Pacific. In other words, in this dynamic system which experiences a strong zonal advection, slow latitudinal transport cannot be neglected when considering the fate of primary production.

[26] The significant standing stocks of marine snow with respect to phytoplankton biomass may be explained by different turnover times of these two particulate pools. While phytoplankton biomass turns over rapidly, the slower formation and decay processes of amorphous particles allows the accumulation of substantial mass. This may also indicate that the consumption of marine snow is rather low.

[27] **Acknowledgments.** We thank M. R. Landry and M. Youngbluth for helpful comments, the crew of R/V *Atalante* from IFREMER for the efficient technical assistance and the IRD, INSU-CNRS and the EURAPP EC program under contract MAS-CT98-061 for financial support.

References

Alldredge, A. L., The carbon, nitrogen and mass content of marine snow as function of aggregate size, *Deep Sea Res., Part I*, *45*, 529–541, 1998.

Alldredge, A. L., and C. C. Gotschalk, In situ settling behavior of marine snow, *Limnol. Oceanogr.*, *33*, 339–351, 1988.

Alldredge, A. L., and C. C. Gotschalk, Direct observations of the flocculation of diatom blooms: Characteristics, settling velocity and formation of diatom aggregates, *Deep Sea Res., Part A*, *36*, 159–171, 1989.

Alldredge, A. L., and M. W. Silver, Characteristics, dynamics and significance of marine snow, *Prog. Oceanogr.*, *20*, 41–82, 1988.

Asper, V. L., Measuring the flux and sinking speed of marine snow aggregates, *Deep Sea Res., Part A*, *34*, 1–17, 1987.

Brown, S., M. R. Landry, J. Neveux, and C. Dupouy, Microbial community abundance and biomass along a 180° transect in the equatorial Pacific during an ENSO cold phase, *J. Geophys. Res.*, *108*(C12), 8139, doi:10.1029/2001JC000817, in press, 2003.

Chavez, F. P., Size distribution of phytoplankton in the central and eastern tropical Pacific, *Global Biogeochem. Cycles*, *3*, 27–35, 1989.

Chavez, F. P., and R. T. Barber, An estimate of new production in the equatorial Pacific upwelling, *Deep Sea Res., Part A*, *34*, 1229–1243, 1987.

Chavez, F. P., and J. R. Toggweiler, Physical estimates of global new production: The upwelling contribution, in *Upwelling in the Ocean: Modern Processes and Ancient Records*, edited by C. P. Summerhayes et al., pp. 313–320, John Wiley, Hoboken, N. J., 1995.

Dam, H. G., X. Zhang, M. Butler, and M. R. Roman, Mesozooplankton grazing and metabolism at the equator in the central Pacific: Implications for carbon and nitrogen fluxes, *Deep Sea Res., Part II*, *42*, 735–755, 1995.

Dunne, J. P., J. W. Murray, M. Rodier, and D. A. Hansell, Export flux in the western and central equatorial Pacific: Zonal and temporal variability, *Deep Sea Res., Part I*, *47*, 901–936, 2000.

Eldin, G., and M. Rodier, Ocean physics and nutrient fields along 180° during an ENSO cold phase, *J. Geophys. Res.*, *108*(C12), 8137, doi:10.1029/2000JC000746, in press, 2003.

Fowler, S., and G. A. Knauer, Role of large particles in the transport of elements and organic compounds through the oceanic water column, *Prog. Oceanogr.*, *16*, 147–194, 1986.

Gardner, W. D., and I. D. Walsh, Distribution of macroaggregates and fine-grained particles across a continental margin and their potential role in fluxes, *Deep Sea Res., Part A*, *37*, 401–411, 1990.

Gaudy, R., G. Champalbert, and R. Le Borgne, Feeding and metabolism of mesozooplankton in the equatorial Pacific high-nutrient, low chlorophyll zone along 180°, *J. Geophys. Res.*, *108*(C12), 8144, doi:10.1029/2000JC000743, in press, 2003.

Gorsky, G., C. Aldorf, M. Kage, M. Picheral, Y. Garcia, and J. Favole, Vertical distribution of suspended aggregates determined by a new Underwater Video Profiler, *Ann. Inst. Oceanogr.*, *68*, 13–23, 1992.

Gorsky, G., M. Picheral, and L. Stemmann, Use of the Underwater Video Profiler for the study of aggregate dynamics in the north Mediterranean, *Estuarine Coastal Shelf Sci.*, *50*, 121–128, 2000.

Gorsky, G., L. Prieur, I. Taupier-Letage, L. Stemmann, and M. Picheral, Large particulate matter (LPM) in the western Mediterranean. I - LPM distribution related to hydrodynamics, *J. Mar. Syst.*, *33–34*, 289–311, 2002.

Honjo, S. K., K. W. Doherty, Y. C. Agrawal, and V. L. Asper, Direct optical assessment of large amorphous aggregates (marine snow) in the deep ocean, *Deep Sea Res., Part A*, *31*, 67–76, 1984.

Jackson, G. A., R. Maffione, D. K. Costello, A. L. Alldredge, B. Logan, and H. G. Dam, Particle size spectra between 1 μm and 1 cm at Monterey Bay determined using multiple instruments, *Deep Sea Res., Part I*, *44*, 1739–1767, 1997.

Kadko, D. C., L. Washburn, and B. Jones, Evidence of subduction within cold filaments of the northern California coastal transition zone, *J. Geophys. Res.*, *96*, 14,909–14,926, 1991.

Kiorboe, T., P. Tiselius, B. Mitchell-Innes, J. L. S. Hansen, A. W. Visser, and X. Mari, Intensive aggregate formation with low vertical flux during an upwelling-induced diatom bloom, *Limnol. Oceanogr.*, *43*, 104–116, 1998.

Landry, M. R., J. Constantinou, and J. Kirshtein, Microzooplankton grazing in the central equatorial Pacific during February and August, 1992, *Deep Sea Res., Part II*, *42*, 657–671, 1995.

Le Borgne, R., and M. R. Landry, EBENE: A JGOFS investigation of plankton variability and trophic interactions in the equatorial Pacific (180°), *J. Geophys. Res.*, *108*(C12), 8136, doi:10.1029/2001JC001252, in press, 2003.

Le Borgne, R., G. Champalbert, and R. Gaudy, Mesozooplankton biomass and composition in the equatorial Pacific along 180°, *J. Geophys. Res.*, *108*(C12), 8143, doi:10.1029/2000JC000745, 2003.

Le Bouteiller, A., J. Blanchot, and J. Neveux, Primary production, new production, and growth rate in the equatorial Pacific: Changes from mesotrophic to oligotrophic regime, *J. Geophys. Res.*, *108*(C12), 8141, doi:10.1029/2000JC000914, in press, 2003.

Legendre, L., and P. Legendre, *Ecologie*, vol. 1, *Le Traitement Multiple des Données Écologiques*, *Coll. Ecol.*, vol. 1, 260 pp., Masson, Québec, Canada, 1984.

MacIntyre, S., A. L. Alldredge, and C. C. Gotschalk, Accumulation of marine snow at density discontinuities, *Limnol. Oceanogr.*, *40*, 449–468, 1995.

Picaut, J., M. Ioualalen, C. Menkes, T. Delcroix, and M. J. McPhadden, Mechanism of the zonal displacement of the Pacific warm pool: Implication for ENSO, *Science*, *274*, 1486–1489, 1996.

Radenac, M.-H., and M. Rodier, Nitrate and chlorophyll distributions in relation to thermohaline and current structures in the western tropical Pacific during 1985–1989, *Deep Sea Res., Part II*, *43*, 725–752, 1996.

Send, U., J. Font, G. Krahmann, C. Millot, M. Rhein, and J. Tintore, Recent advances in observing the physical oceanography of the western Mediterranean Sea, *Prog. Oceanogr.*, *44*, 37–64, 1999.

Stemmann, L., M. Picheral, and G. Gorsky, Diel variation in the vertical distribution of particulate matter (>0.15 mm) in the NW Mediterranean Sea investigated with the Underwater Video Profiler, *Deep Sea Res., Part I*, *47*, 507–534, 2000.

Tans, P. P., I. Y. Fung, and T. Takahashi,Observationalconstraints on the global atmospheric CO_2 budget, *Science*, *247*, 1431–1438, 1990.

Videau, C., A. Sournia, L. Prieur, and M. Fiala, Phytoplankton and primary production characteristics at selected sites in the geostrophic Almeria-Oran front system (SW Mediterranean Sea), *J. Mar. Syst.*, *5*, 235–250, 1994.

Walsh, I. D., and W. D. Gardner, A comparison of aggregates profiles with sediment trap fluxes, *Deep Sea Res., Part A*, *39*, 1817–1834, 1992.

Walsh, I. D., W. D. Gardner, M. J. Richardson, S. P. Chung, C. A. Plattner, and V. L. Asper, Particle dynamics as controlled by the flow field of the eastern equatorial Pacific, *Deep Sea Res., Part II*, *44*, 2025–2047, 1997.

G. Gorsky, M. Picheral, and L. Stemmann, Observatoire Océanologique, LOV, CNRS/UPMC, BP 28, 06230 Villefranche sur mer, France. (gorsky@obs-vlfr.fr; picheral@obs-vlfr.fr)

R. Le Borgne, Centre IRD, B.P. A5, Nouméa Cédex, New Caledonia.